Coded Noncoherent Communication with Amplitude/Phase Modulation: From Shannon Theory to Practical Architectures

Noah Jacobsen, *Member, IEEE*, and Upamanyu Madhow, *Fellow, IEEE*

***Abstract*—We develop bandwidth efficient radio transceivers, using amplitude/phase modulations, for frequency non-selective channels whose time variations are typical of outdoor mobile wireless systems. The transceiver is *noncoherent*, neither requiring pilots for channel estimation and tracking nor assuming prior channel knowledge on the part of the receiver. Serial concatenation of a binary outer channel code with an inner differential modulation code provides a turbo structure that, along with the channel memory, is exploited for joint iterative channel and data estimation. While prior work on noncoherent communication mainly focuses on PSK alphabets, we consider a moderate to high SNR regime in which amplitude/phase constellations are more efficient. First, the complexity of block noncoherent demodulation is reduced to a level that is comparable to coherent receivers. Then, a tool for choosing the constellation and bit-to-symbol mapping is developed by adapting Extrinsic Information Transfer (EXIT) charts for noncoherent demodulation. The recommended constellations differ significantly from standard coherent channel constellations, and from prior recommendations for uncoded noncoherent systems. The analysis shows that standard convolutional codes are nearly optimal when paired with differential amplitude/phase modulation.**

***Index Terms*—Wireless communications, fading channels, noncoherent detection, coding, capacity.**

I. Introduction

We consider time-varying channels with memory, such as those encountered in high data-rate outdoor mobile wireless systems. Methods for the design and analysis of turbo-like coded modulation schemes which approach the information-theoretic limits for such channels are explored. We employ a block fading frequency non-selective channel model, in which the channel scales the transmitted signal by a scalar complex gain which is constant over a block of symbols (referred to as the *channel coherence length* for the length of the block), with the gain chosen independently from block to block. This model facilitates the development of low-complexity noncoherent block demodulation techniques, which implicitly estimate the channel gain and phase on each block, while being amenable to information-theoretic comparisons. More importantly, the block fading model provides a useful framework for transceiver design for existing and projected cellular systems. Such designs can be adapted efficiently to continuous fading channels in which the symbol rate is much greater than the Doppler frequency or residual frequency offset. The frequency non-selective model not only applies to narrowband systems, but also to each subcarrier in a wideband Orthogonal Frequency Division Multiplexed (OFDM) system. In a typical OFDM system, the channel gain can be well modeled as constant over a time-frequency block whose size depends on the channel coherence time and coherence bandwidth.

Summary of Results: In order to control the implementation complexity, we restrict attention to serial concatenation of a binary convolutional code with differential modulation over a two-dimensional constellation. The main steps in our design approach are as follows:

(a) Independent and identically distributed (i.i.d.) inputs chosen from an appropriate two-dimensional constellation are shown to approach the Shannon capacity of the (input power constrained) block fading channel. As expected, at moderately large Signal-to-Noise Ratio (SNR), Phase Shift Keying (PSK) cannot attain Shannon capacity and amplitude/phase modulation, also termed QAM,[1] is required. However, the capacity is insensitive to the constellation shape. For example, offset PSK rings, rectangular QAM, and aligned PSK rings are close to capacity, as long as their shape parameters are optimized as a function of the SNR.

(b) We employ differential modulation over amplitude and phase, with Gray-like bit-maps, in a straightforward generalization of differential PSK. An approximate Maximum A Posteriori (MAP) block noncoherent demodulation scheme, with complexity comparable to coherent demodulation, is used to provide soft information to the outer decoder. Block demodulation is necessary because standard two-symbol differential demodulation incurs a loss for two-dimensional constellations. However, brute force approaches to block noncoherent demodulation have exponential complexity in the block length, while our soft decision scheme has linear complexity.

(c) Standard turbo iterations between the outer decoder and

Paper approved by N. C. Beaulieu, the Editor for Wireless Communication Theory of the IEEE Communications Society. Manuscript received November 4, 2004; revised July 22, 2005 and March 11, 2008.

This work was supported in part by Motorola and by the University of California Discovery program.

N. Jacobsen is with Alcatel-Lucent, Murray Hill, NJ 07974 USA (e-mail: jacobsen@alcatel-lucent.com). This work was performed while with the Dept. of Electrical and Computer Engineering, University of California, Santa Barbara, CA 93106 USA.

U. Madhow is with the Dept. of Electrical and Computer Engineering, University of California, Santa Barbara, CA 93106 USA (e-mail: madhow@ece.ucsb.edu).

Digital Object Identifier 10.1109/TCOMM.2008.040684

[1] We use the term QAM for any amplitude/phase constellation, even though the constellations we ultimately recommend differ in shape from QAM alphabets used in coherent systems.

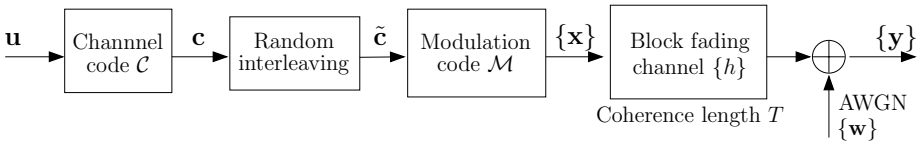

Fig. 1. Transmitter structure and channel model.

the inner noncoherent demodulator work well, as expected. However, unlike the Shannon capacity, the performance is sensitive to constellation shape. For example, aligned PSK rings constellations perform much better than offset PSK rings constellations for the differential bit maps that we use.

(d) An EXIT analysis, modified to account for non-Gaussian soft output from the noncoherent demodulator, is employed to explain the simulation results. In particular, it is shown that aligned PSK rings have an EXIT curve that completely dominates that of offset PSK rings, assuming a differential bit map in phase and amplitude.

Relation to Prior Work: The standard approach to wireless transceiver design is to estimate the channel using pilots, and to then employ coherent demodulation assuming that the channel estimates are perfect. There are two main drawbacks of this approach: the overhead required for pilots to accurately track rapid channel variations is a significant fraction of the available bandwidth; and channel estimates based solely on the pilots are suboptimal, since they do not exploit the bulk of the transmitted energy, which is in the data. A number of recent papers [1], [2], [3], [4] consider the alternative of turbo noncoherent communication, with iterative joint estimation of the channel and data (which does not need pilots, but can exploit them if available).[2] This body of work, especially [4], is the starting point for this paper, which adopts the same basic transceiver architecture: an outer binary code, serially concatenated with a modulation code amenable to noncoherent demodulation. However, while prior work focuses on lower SNR regimes and employs PSK constellations, we are able to approach capacity for larger SNRs by using amplitude/phase modulation. The key to accomplishing this is developing a low-complexity implementable technique for noncoherent block demodulation with soft decisions. While recent results [5] have shown the surprising result that ML or MAP demodulation can be achieved with polynomial complexity, these methods are still too computationally demanding for typical applications, in contrast to the linear complexity of coherent demodulation. In past work on block noncoherent demodulation with PSK alphabets [4], [6], [7], joint channel and data estimation is accomplished by quantizing the channel phase into bins, in conjunction with a simple energy-based amplitude estimator, and then using parallel coherent demodulators for each bin. However, the amplitude estimator in [4] does not work when the signal amplitude varies due to the use of Quadrature Amplitude Modulation (QAM) constellations. Furthermore, maintaining a large number of phase bins implies that the complexity of block noncoherent demodulation is still significantly larger (Q times larger, where Q is the number of phase bins) than that of coherent demodulation. These shortcomings are addressed in this paper by providing a more sophisticated amplitude estimator that is bootstrapped with conventional two-symbol differential detection, and by reducing the number of phase bins to two based on feedback from the outer decoder after the first iteration.

The capacity of the block fading channel was computed by Marzetta and Hochwald [8]. Their result can be interpreted to indicate that, for moderate and low SNRs, and reasonable channel coherence lengths, independent and identically distributed (i.i.d.) Gaussian inputs are near-optimal. Chen *et al.* [4] provide information-theoretic computations showing that this capacity can be approached by the use of standard PSK and QAM constellations (see also [9] for capacity computations for the block phase noisy channel). Our capacity computations are based on the techniques of [4], [8].

Outline: The remainder of the paper is organized as follows. The guidance from Shannon-theoretic computations is summarized in Section II. Receiver processing is described in Section III. Section IV describes the EXIT analysis for our scheme. This, together with simulations of coded performance, is used to guide constellation design in Section V and code choice in Section VI. Finally, Section VII provides discussion supported by further numerical results.

II. Channel Model and Encoding Strategy

Figure 1 depicts the complex baseband transmitter and channel model. The code block length is much larger than the channel coherence length, which provides the time diversity required to approach the ergodic capacity of the block fading channel. The information sequence $\mathbf{u}$ is mapped to codeword $\mathbf{c}$ of the binary channel code $\mathcal{C}$ and pseudo-randomly permuted to the code-symbol sequence $\tilde{\mathbf{c}} = \{c[n]\}$. With the cardinality of the modulation alphabet, $\mathcal{A}$, equal to M, the code symbol $c[n]$ represents $m = \log_2(M)$ permuted code-bits which modulate the nth channel symbol, $x[n]$. Codewords in the modulation code, $\mathbf{x} \in \mathcal{M}$, belong in the T-fold product of the symbol alphabet $\mathcal{A}^T$.

Block fading model: The channel is modeled as constant over disjoint blocks of T symbols, where T is the coherence length. Channel gains for different blocks are modeled as i.i.d. Letting $\mathbf{x}$ denote a block of T transmitted symbols, the block of received symbols is given by

$$\mathbf{y} = h\mathbf{x} + \mathbf{w}, \tag{1}$$

where the channel gain $h = ae^{j\theta}$ is a zero-mean, unit-variance proper complex Gaussian random variable, denoted, $h \sim \mathcal{CN}(0,1)$. This is the Rayleigh fading model, where the channel amplitude, a, is Rayleigh, and channel phase, θ, is uniform over $[0, 2\pi]$; and a and θ are independent. The

[2]See [5] for pilot-aided systems in which feedback from the decoder is employed to refine pilot-based channel estimates.

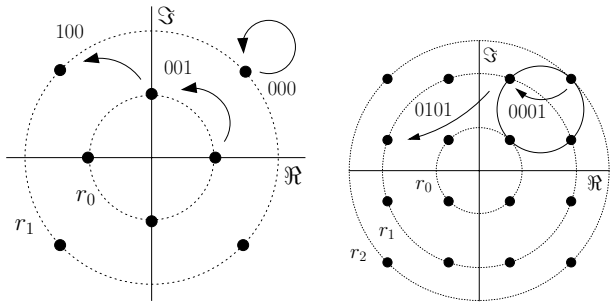

(a) 8-QAM: Offset PSK rings (b) 16-QAM: Lattice

Fig. 2. Conventional AWGN constellations with differential Gray-like bit-mappings.

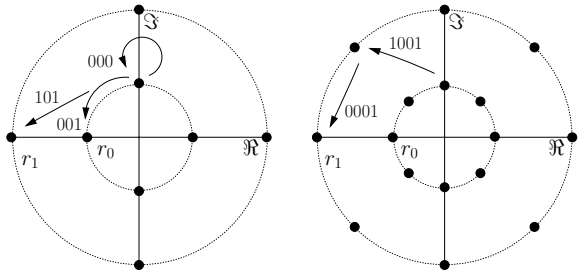

(a) 8-QAM: Aligned rings (b) 16-QAM: Aligned rings

Fig. 3. QAM constellations based on aligned concentric PSK rings and Gray-like bit-mappings outperform conventional AWGN constellations in coded noncoherent systems.

additive noise vector, $\mathbf{w}$, is Gaussian, $\mathcal{CN}(0, 2\sigma^2\mathbf{I}_T)$, where $\mathbf{I}_T$ stands for the $T \times T$ identity matrix. The Rayleigh fading model is equivalently defined by the conditional probability density function (PDF) of the received symbols given the transmitted symbols [8]:

$$f(\mathbf{y}|\mathbf{x}) = \frac{\exp\{-\mathrm{tr}([2\sigma^2\mathbf{I}_T + \mathbf{x}\mathbf{x}^{\mathrm{H}}]^{-1}\mathbf{y}\mathbf{y}^{\mathrm{H}})\}}{\pi^T \det(2\sigma^2\mathbf{I}_T + \mathbf{x}\mathbf{x}^{\mathrm{H}})}. \quad (2)$$

The ergodic capacity of the block fading channel under various input constraints can be computed using the model (2).

Block fading approximation to continuously varying channel: Since there is no absolute amplitude and phase reference within a block, the signals over a block of length T live in a $(T-1)$-dimensional manifold [10], which costs a rate penalty of $1/T$. This can be intuitively interpreted as resulting from the use of one symbol in the block as a amplitude/phase reference, or pilot (whether or not this is explicitly done). However, in practice, this rate loss can be avoided when applying the block fading model to a continuously varying channel, by overlapping successive blocks by one symbol. Thus, by including the last symbol of the previous block as the first symbol of the current block, we have $T-1$ new channel uses required for signaling in a $(T-1)$-dimensional manifold. Of course, when applying the block fading approximation to a continuously varying model, there are two sources of performance loss: first, the approximation error in modeling the channel gain as constant over a block, and second, the loss due to not exploiting the continuity of the channel in adjacent blocks explicitly for channel estimation. However, these losses are expected to be small if the block length T is chosen appropriately, and the operating SNR is not extremely high.

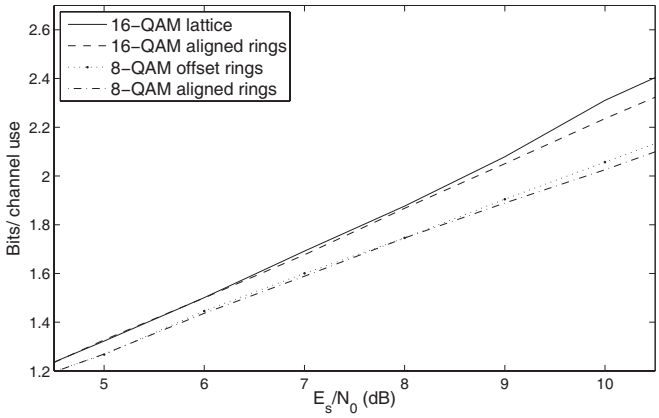

Fig. 4. Noncoherent capacity of 8- and 16-QAM constellations.

A. Differential Modulation for Amplitude/Phase Constellations

The bits from the outer binary code are interleaved, and fed to a differential modulator, using a generalization of differential PSK to amplitude/phase modulation. As depicted in Figures 2 and 3, we consider amplitude/phase constellations of three basic shapes: offset PSK rings, aligned PSK rings, and lattice QAM. Offset PSK rings consist of concentric rings such that signal points are placed with even spacing around each ring, but the placement is offset across rings. In aligned PSK rings, the placement of signal points in different rings is aligned along rays emanating from the origin. Lattice QAM refers to rectangular point placement, which is a common choice for coherent communication.

Figure 4 shows the results of Shannon capacity computations using the techniques of [8], [4], based on the channel model (2). These show that both lattice QAM and aligned PSK rings (with ratio of radii optimized) approach the capacity of the block fading channel for moderately high SNR. For example, in our coded simulations, an information rate of 1.8 bits per channel symbol is achieved using 16-QAM constellations. At this rate, the 16-QAM capacity as measured in Figure 4 is within 0.5 dB of the unconstrained capacity reported in [4]. On the other hand, simulations show that aligned PSK rings perform much better for our coded modulation scheme. Thus, Shannon theory provides only rough guidance on constellation choice, and design techniques that provide guidance on constellation optimization for a specific coded modulation strategy are required. We demonstrate that a suitable adaptation of EXIT chart analysis is useful for this purpose.

III. Noncoherent Receiver Processing

We first provide an overview of the receiver iterative processing which involves soft information exchange between the outer binary decoder and an inner block noncoherent demodulator. The outer decoder employs a Soft-Input, Soft-Output (SISO) BCJR algorithm [11] as a building block. This section is mainly devoted to describing the SISO noncoherent demodulator, which has to handle the unknown channel. The key

challenge is the reduction of complexity to levels comparable with that of symbol-by-symbol coherent demodulation. Block noncoherent demodulation can be viewed as joint estimation of the data and the channel (which in our case is a complex scalar modeled as constant over each block). We estimate the channel amplitude for a block using a bootstrap phase which employs classical two-symbol differential demodulation. The uncertainty regarding channel phase is handled by quantizing the unknown phase into a discrete set of hypotheses. For each such phase bin, the BCJR algorithm (that accounts for the memory due to inner differential modulator) can perform coherent demodulation using the channel amplitude and phase estimate. The final soft outputs are obtained by averaging over the phase bins. After the first iteration, the number of phase bins is reduced to two by exploiting the information from the decoder, thus reducing the complexity of the noncoherent demodulator to twice that of coherent demodulation.

A. Bootstrap amplitude estimation

An amplitude estimator, whose complexity is linear in the product of the number of amplitude levels and size of the modulation alphabet, is described. An amplitude/phase constellation based on concentric PSK rings is assumed, but the estimate is readily generalized. The polar representation of the nth transmitted symbol is defined as $x[n] = r[n]\exp(j\omega[n])$, where $r[n] \in \mathcal{R}$ denotes the amplitude level of the nth symbol, and $\omega[n]$ is the phase. Conventional two-symbol likelihoods do not require channel knowledge, and are used to obtain a posterior distribution on $r[n]$. These amplitude posteriors are then used to compute an energy based estimate of a. Note that this bootstrap phase is not required of constant-amplitude PSK signals.

The vector of two received symbols is

$$\begin{aligned}\mathbf{y}[n] &= \begin{bmatrix} y[n-1] \\ y[n] \end{bmatrix} = h \begin{bmatrix} r[n-1] \\ r[n]\exp(j\omega[n]) \end{bmatrix} + \begin{bmatrix} w[n-1] \\ w[n] \end{bmatrix} \\ &= h\mathbf{x}[n] + \mathbf{w}[n].\end{aligned}$$

Note that the phase of the $(n-1)$th symbol is factored into the channel without changing the density function. The two-symbol conditional log-likelihood is given by

$$\log f(\mathbf{y}[n]|\mathbf{x}[n]) = \frac{1}{2\sigma^2}\frac{\left|\mathbf{y}[n]^{\mathrm{H}}\mathbf{x}[n]\right|^2}{\|\mathbf{x}[n]\|^2 + 2\sigma^2} - \log(\|\mathbf{x}[n]\|^2 + 2\sigma^2) + a,$$

where a is a constant that does not depend on $\mathbf{x}[n]$. Defining the posterior probability of the nth symbol amplitude $r[n]$ as μ_n, we have

$$\mu_n(r) = Pr(r[n] = r|\mathbf{y}[n+1]) \propto \sum_{x \in \mathcal{R}\times\mathcal{A}: r[n]=r} f(\mathbf{y}[n+1]|\mathbf{x}[n+1] = x).$$

The energy based channel amplitude estimate, $\hat{a}$, is computed with (3), where T denotes the coherence length of the channel and $\mathbf{y}$ is a length T block of symbols.

$$\hat{a}^2 = \max\left\{0, \frac{\|\mathbf{y}\|^2 - 2T\sigma^2}{\sum_{n=1}^{T}\sum_{r\in\mathcal{R}}\mu_n(r)r^2}\right\} \tag{3}$$

B. Phase quantization

We first repeat an argument from [4] (and prior references therein) to illustrate how to minimize the complexity entailed by phase quantization. Consider a PSK constellation with differential modulation. The absolute phase of a noiseless received symbol is the sum of an initial phase and the phase change corresponding to the bits indexing the transition. The initial phase is the sum of the channel phase and the phase of the previous symbol. If ϕ is the smallest angle by which the constellation can be rotated while maintaining the same signal points (e.g., $\phi = \frac{\pi}{2}$ for QPSK), we can synthesize any initial phase by choosing the channel phase in the interval $[0, \phi]$, and choosing the previous symbol appropriately. Thus, for block differential demodulation, instead of quantizing the channel phase over the entire interval $[0, 2\pi]$, we can quantize it over an interval $[0, \phi]$, simply by allowing the first symbol in the block to take arbitrary values.

The preceding argument generalizes to differential modulation with amplitude/phase constellations, as long as they satisfy the following ϕ-rotational invariance property.

ϕ-rotational invariance: Rotational invariance applies to amplitude/phase constellations that are rotationally symmetric in the following sense: There exists an angle, ϕ, for which $e^{jk\phi}x \in \mathcal{A}$, for all $x \in \mathcal{A}$ and $k \in \mathbb{Z}$. If, further, the differential bit-to-symbol mapping, $\nu : \{0,1\}^m \times \mathcal{A} \to \mathcal{A}$, satisfies the condition $\nu(c[n], e^{jk\phi}x[n-1]) = e^{jk\phi}\nu(c[n], x[n-1])$, $k \in \mathbb{Z}$, the modulation code is referred to as ϕ-rotationally invariant.

All of the examples considered in this paper satisfy the preceding property with nontrivial ϕ (i.e., for $\phi < 2\pi$). The 16-QAM lattice constellation has $\phi = \pi/2$, while 16-QAM with aligned PSK rings has $\phi = \pi/4$.

By ϕ-rotational invariance, the APPs averaged over the unknown channel phase can be approximated by a discrete average of the APPs produced by coherent demodulation over Q phase bins quantizing the interval $[0, \phi]$, as follows:

$$\begin{aligned}Pr(c[n]|\mathbf{y}, a = \hat{a}) &= \frac{L}{2\pi}\int_0^{\phi} d\theta\ Pr\big(c[n]|\mathbf{y}, h = \hat{a}\exp(j\theta)\big) \\ &\approx \frac{1}{Q}\sum_{q=0}^{Q-1} Pr\big(c[n]|\mathbf{y}, h = \hat{a}\exp(j\phi q/Q)\big). \end{aligned} \tag{4}$$

where $L = 2\pi/\phi$.

Maps that do not have the rotational invariance property (e.g. Block-DPSK [4]) require quantization over the full unit circle, and thus an L-fold increase in complexity.

The BCJR algorithm used for coherent demodulation on each phase bin views the differential bit map ν as a unit-rate/memory recursive convolutional code. To each trellis edge, e, corresponds an initial and final state, $s^I(e)$ and $s^F(e)$, input code bits, $c(e)$, and output channel symbol, $x(e)$. The coherent posteriori probability, $p_n(c|h) = \log Pr(c[n] = c|\mathbf{y}, h)$, of the code symbol, $c[n]$, is computed in the logarithmic domain, using

$$p_n(c|h) = \max_{e:c(e)=c}{}^{\star}\left(\alpha_{n-1}(s^I(e)) + \gamma_n(e) + \beta_n(s^F(e))\right).$$

The forwards/backwards recursions for α_n and β_n are defined

as follows (h denotes the channel):

$$\alpha_n(x) = \max_{e:s^F(e)=x}{}^{\star} \left(\gamma_n(e) + \alpha_{n-1}(s^I(e))\right),$$
$$\alpha_1(x) = \sigma^{-2}\,\Re\langle y[1], hx\rangle, \quad x \in \mathcal{A}.$$
$$\beta_n(x) = \max_{e:s^I(e)=x}{}^{\star} \left(\gamma_{n+1}(e) + \beta_{n+1}(s^F(e))\right),$$
$$\beta_T(x) = -\log_2(M), \quad x \in \mathcal{A}.$$

The *max-star* function above is the usual logarithmic summation, defined as follows:

$$\max_{Z\in\mathcal{F}}{}^{\star}(Z) = \log\Big(\sum_{Z\in\mathcal{F}} e^Z\Big).$$

The branch metric $\gamma_n(e)$ of edge e is given by:

$$\gamma_n(e) = \pi_n(c(e)) + \sigma^{-2}\,\Re\langle y[n], hx(e)\rangle,$$

where prior probabilities of the code-symbols, $\pi_{\mathcal{M}} = \{\pi_n\}$, $\pi_n(c) = \log Pr(c[n] = c)$, are initially uniform and then set by the outer decoder through turbo processing.

Extrinsic posteriors, $\lambda_{\mathcal{M}} = \{\lambda_n\}$, are then computed via (4), which in the log-domain translates to

$$\lambda_n(c) = \log\left(Pr(c[n] = c|\mathbf{y}, a = \hat{a})\right) - \pi_n(c)$$
$$\approx \max_{q\in\mathcal{Q}}{}^{\star}\left(\, p_n(c|\hat{a}\exp(j\phi q/Q)\,\right) - \pi_n(c).$$

This yields extrinsic APPs for the outer decoder.

C. Phase branch pruning

Noncoherent demodulation implemented using coherent demodulation over Q phase bins incurs a Q-fold complexity increase relative to coherent systems. Simulations show, however, that a genie-based system, which uses only the phase bin which is closest to the true channel phase, yields comparable performance to Q-fold averaging. We therefore investigate a reduced complexity implementation, which prunes the number of phase branches, especially in later iterations when we have soft information from the outer decoder. For this purpose, a generalized likelihood ratio test (GLRT) approach for phase branch selection is introduced, where the observation is the received signal and extrinsic information from the decoder, and the parameters to be estimated are the channel and the transmitted data.

The GLRT operates with the joint likelihood function, $f(\Gamma|\mathbf{x}, h)$, of the "observation" $\Gamma = \{\mathbf{y}, \pi_{\mathcal{M}}\}$, given $\mathbf{x}$ and h. Phase estimation with the GLRT involves maximization of the likelihood function first over transmitted symbol vectors and then over the quantized channel phase (5). The GLRT is is thus viewed as a joint maximum likelihood estimate of θ and $\mathbf{x}$ based on the observation Γ.

$$\hat{\theta}_{GLRT}(\gamma) = \arg\max_{q\in\mathcal{Q}}\max_{\mathbf{x}\in\mathcal{M}} f(\gamma|\mathbf{x}, \hat{a}\exp(j\phi q/Q)). \quad (5)$$

The inner maximization, $f(\gamma|\hat{\mathbf{x}}_q, \hat{a}\exp(j\phi q/Q))$, represents the conditional probability of the maximum likelihood sequence estimate (MLSE), $\hat{\mathbf{x}}_q$, on the qth phase trellis. We propose to estimate the likelihood of the MLSE sequence, typically computed with the Viterbi algorithm, with the forward recursion of BCJR algorithm, with $\max_{x\in\mathcal{A}}(\alpha_T(x)|h = \hat{a}\exp(j\phi q/Q))$. This approximation is found to be accurate in numerical comparisons. Since $\{\alpha_T\}$ are computed in the trellis processing, they are a natural choice for measuring the reliability of soft decisions output by each phase branch. This metric, when used to choose the best two phase branches after the first receiver iteration (this is found to provide much better performance than simply choosing the best branch), yields performance within 0.1 dB to that of averaging over all phase bins. Thus, after the first iteration, noncoherent block demodulation requires only twice as many BCJR computations as coherent demodulation of the same code.

IV. EXIT functions of noncoherent codes

We study the convergence behavior of iterative noncoherent demodulation and decoding via extrinsic information transfer (EXIT) charts [12], [13]. The EXIT chart of a noncoherent code is a graphical description of iterative noncoherent demodulation and decoding, portraying the mutual information between decoder messages communicated and code-symbols estimated, as evolved through turbo-processing. Consider first the inner modulation code, that maps the code bits, $\mathbf{c} = \{c_k\}$, to channel symbols. The noncoherent block demodulator computes posterior probabilities, $\Lambda_{\mathcal{M}} = \{\Lambda_k\}$,

$$\Lambda_k = \log\frac{Pr(c_k = 0|\Pi_{\mathcal{M}}, \{\mathbf{y}\})}{Pr(c_k = 1|\Pi_{\mathcal{M}}, \{\mathbf{y}\})} - \Pi_k,$$

where $\Pi_{\mathcal{M}} = \{\Pi_k\}$ denotes the code-bit priors, with $\Pi_k = \log\frac{Pr(c_k=0)}{Pr(c_k=1)}$. The *EXIT function* A, for modulation code $\mathcal{M}$, describes the mutual information of the code-bits and APPs, $a^{out} = I(\mathbf{c}; \Lambda_{\mathcal{M}})$, as a function of the input mutual information (of the code bits and priors), $a^{in} = I(\mathbf{c}; \Pi_{\mathcal{M}})$, and channel SNR, according to $a^{out} = A(a^{in}, \text{SNR})$. Conditional probability density functions of decoder priors are often well-modeled as i.i.d., with a single-parameter family of Gaussian densities [13]:

$$\Pi_k \sim \mathcal{N}(\pm 2\gamma, 4\gamma),\ \gamma \in [0, \infty). \quad (6)$$

This model for the code-bit priors can be interpreted as log-likelihoods that arise from BPSK transmission, $\{(-1)^{c_k}\}$, of codeword $\{c_k\}$, over an AWGN channel at SNR γ. In this case, a^{in} can be computed with the simplified estimate (see [13]),

$$a^{in} = E\left[1 - \log\big(1 + \exp(\Pi_k)\big)|c_k = 1\right]. \quad (7)$$

With $\mathcal{M}$ discrete, we have $A : [0, 1] \to [0, 1]$, and the parameter γ is varied to generate a^{in} over the support of A. The output mutual information, a^{out}, is computed empirically by measuring conditional probability density functions of Λ_k that are generated by the decoder fed with $\Pi_{\mathcal{M}}$ as in (6).

We next consider the EXIT function, B, of the outer channel code, $\mathcal{C}$. The APP decoder for $\mathcal{C}$ computes posterior probabilities of the code-bits, $\Lambda_{\mathcal{C}}$, with the priors $\Pi_{\mathcal{C}}$ (permuted extrinsics from APP demodulation). Letting $b^{in} = I(\mathbf{c}, \Pi_{\mathcal{C}})$ and $b^{out} = I(\mathbf{c}, \Lambda_{\mathcal{C}})$ denote input and output decoder mutual information, the decoder EXIT function is given by $b^{out} = B(b^{in})$. In many cases, log-APPs produced by the outer channel decoder, e.g. the convolutional decoder, are well modeled as Gaussian. Then, a^{out}, the demodulator output mutual information, is accurate when computed empirically

from demodulator APPs that are generated from the priors (6). However, we find that the extrinsic information, $\Lambda_{\mathcal{M}}$, produced with block noncoherent demodulation does not fit a Gaussian model, due to the relatively short channel coherence length, so that estimates of the decoder EXIT function based on Gaussian priors do not accurately model density evolution for the noncoherent demodulator.

The following modified EXIT chart technique is used to compute the decoder EXIT function. Since decoder priors are de-interleaved code-symbol posteriors from the demodulator, the following two-stage approach is proposed: First, Gaussian code-bit priors are noncoherently demodulated; demodulator input mutual information, a^{in}, is computed with (7) and output mutual information, a^{out}, is estimated empirically. Then, the resulting extrinsic (de-interleaved) code-bit APPs are sent to the decoder as priors, $\Pi_{\mathcal{C}}$, now accurately modeling the priors observed from noncoherent processing. Decoder output mutual information is computed empirically from the resulting decoder extrinsics, $\Lambda_{\mathcal{C}}$. The parameter γ is varied to generate a range of priors through the demodulator as described.

The sequences of output mutual information values that are realized through iterative demodulation and decoding are denoted $\{a_k^{out}\}$, $\{b_k^{out}\}$, respectively. The following properties of EXIT charts are relevant to the code and constellation design problem.

Property 1: The information Bit Error Rate (BER) approaches zero if and only if the decoder output sequence $\{b_k^{out}\}$ converges to one. An equivalent condition for code convergence is given by $B^{-1} < A$. Final decoder output mutual information values less than one give rise to an error floor.

Property 2: Channel SNR provides an ordering of demodulator EXIT functions such that if A and A' are measured at SNRs τ and τ', respectively, with $\tau < \tau'$, then $A \leq A'$. The *convergence threshold* of a code is the SNR threshold, τ, for which the output mutual information converges to one if and only if SNR$> \tau$.

Property 3: The area property of trellis decoders: $\int_0^1 B^{-1} = r_{\mathcal{C}}$, where $r_{\mathcal{C}}$ denotes the code rate. This property, proved only for erasures channels [14], is observed empirically for a wide variety of channels and serves as the basis for EXIT chart based optimization techniques. We show that this property implies that convolutional outer codes are near-optimal when the inner code is unit-rate differential modulation code.

As a rule of thumb, the operating SNR does not affect the shape of the demodulator transfer function but rather its vertical offset. Since the channel decoder does not directly observe channel output, its transfer function is unaffected by SNR. Figure 5 illustrates Property 2 for 16-ary constellations. EXIT chart analysis of noncoherent codes provides a quantitative framework for comparing signal alphabets, outer channel decoders, or complexity reducing techniques without having to simulate BER performance. In particular, Figure 5 shows that 16-QAM based on aligned PSK rings is superior to the 16-QAM lattice constellation over a wide range of SNR.

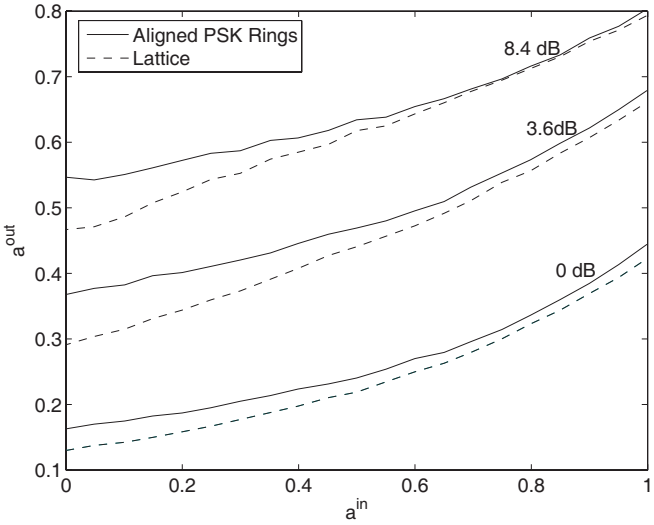

Fig. 5. EXIT functions of 16-ary amplitude/phase constellations.

V. Constellation Design for Coded Noncoherent Modulation

We consider the design of amplitude/phase constellations and bit-to-symbol maps well-suited for turbo noncoherent communication over the Rayleigh block fading channel. The main tools for design and optimization of the modulation codes are noncoherent capacity and modified EXIT chart analysis, where we use the term "noncoherent capacity" for the mutual information attained by various input distributions for noncoherent communication over the block fading channel. Marzetta and Hochwald [8] have shown that the unconstrained noncoherent capacity is achieved by T-dimensional isotropically distributed vectors, with $E[\mathbf{x}^{\mathrm{H}}\mathbf{x}] = T$. This is equivalent to sending i.i.d. Gaussian symbols, with the energy over a block of T symbols normalized to a constant. Intuitively, therefore, suitable modifications of designs similar to those employed for the AWGN channel, for which i.i.d. Gaussian input is optimal, are expected to work for the noncoherent Rayleigh block fading channel. In particular, QAM constellations approximate Gaussian input distributions more closely than PSK, especially for a large number of points. We first consider 16-QAM lattice constellation with differential Gray-like bit maps, as in Figure 2. The bit maps in this case index transitions within and between QPSK sub-constellations within the QAM constellation. However, in simulations of a coded noncoherent system, such lattice QAM constellations, at least in conjunction with the bit maps we have considered, perform poorly, not delivering on the promised gains over PSK. We therefore consider an alternative class of QAM constellations, in the form of aligned PSK rings. These constellations, along with Gray-like bit maps for encoding data in the amplitude and phase transitions, are depicted in Figure 3. The ratios of the radii are optimized using capacity. As discussed, these constellations are found to perform much better than lattice based QAM.

Figure 6 compares the simulated BER of aligned PSK rings constellations with lattice-based 16-QAM and 8-QAM. Standard convolutional codes [15], with a memory of four bits, are employed for an overall data rate of 1.35 bits/channel symbol.

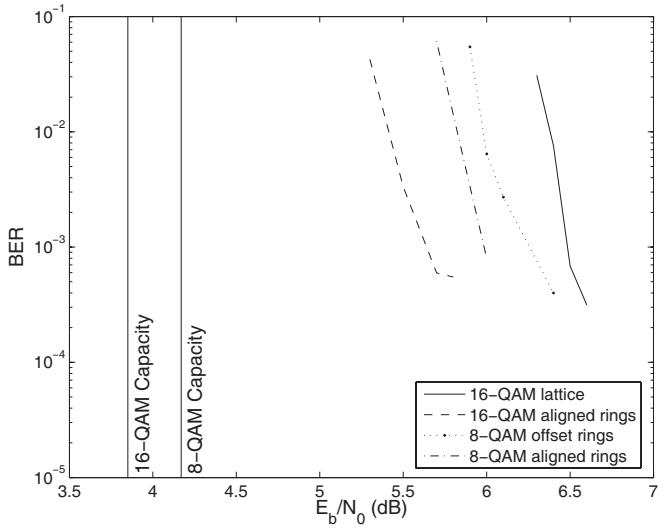

Fig. 6. Coded performance of 8- and 16-QAM constellations.

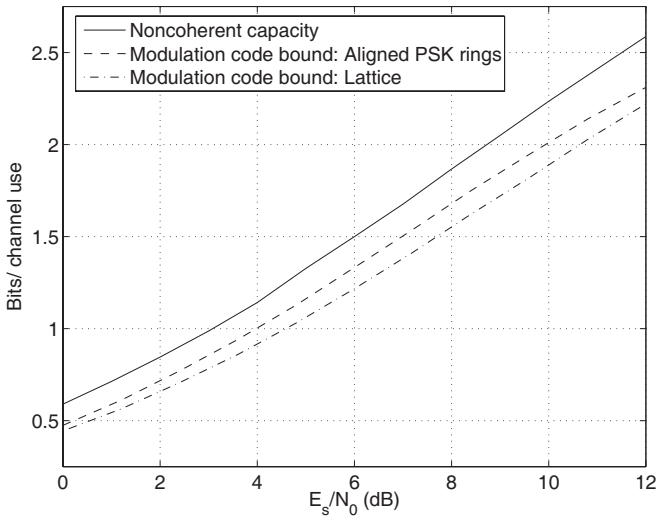

Fig. 7. The modulation code bound for unit-rate differential modulation with aligned PSK rings 16-QAM is about 1 dB from capacity.

The rate-1/2 code (with 8-QAM) has generator polynomial $G = [23\ 35]$ (octal representation). The rate-3/8 code (with 16-QAM) is obtained by randomly puncturing a rate-1/3 mother code with generator polynomial $G = [25\ 33\ 37]$.

The figure shows the gain in using aligned PSK rings over rectangular lattices: 1 dB for 16-ary constellations, and 0.2 dB for 8-ary constellations. It also displays the advantage of constellation expansion with heavier coding: for the same information rate, 16-QAM aligned PSK rings outperform 8-QAM aligned PSK rings by 0.5 dB. This advantage is not realized for poor constellation and bit map choices: the lattice 16-QAM performs significantly worse than the 8-ary constellations at the same information rate.

The advantage of aligned PSK rings is understood via EXIT analysis. Figure 5 shows that, at the same SNR, the EXIT chart for aligned PSK rings 16-QAM is strictly greater than that of lattice 16-QAM with noncoherent block demodulation and Gray-like differential bit maps. This implies that the convergence threshold of any outer code will be larger for lattice 16-QAM. A possible intuitive explanation for the superior performance of aligned rings is as follows. For blocks suffering from poor SNR due to fading, the aligned PSK rings effectively collapse to a more robust PSK constellation. Thus, while the bits encoded in amplitude transitions are difficult to recover, the bits encoded in phase transitions are relatively better preserved. For lattice constellations, on the other hand, all bits are affected adversely in a faded block. As SNR and the coherence length increases, AWGN-like QAM constellations are preferable, for their better nearest neighbor distances. However, this is not the operating regime for the turbo-like system considered here, where we expect a relatively high uncoded BER. Thus, artful coupling of the constellation shape and bit-to-symbol map is the key to designing bandwidth efficient symbol alphabets for noncoherent systems.

Thus far, we have only considered unit-rate rotationally-invariant differential modulation. These simple modulation codes are well-suited to block noncoherent processing for their low-complexity demodulation and bootstrap function. We now wish to quantify the performance penalty, if any, associated with this restriction (e.g., as opposed to using more sophisticated trellis-based rotationally invariant modulation codes) for a serially concatenated system with an outer binary code. To this end, we apply the following theorem, which provides an upper bound on the achievable rate as a function of SNR for a given inner modulation code, as a function of its EXIT curve.

Theorem 1: Modulation code bound. For a fixed inner modulation code with alphabet size M in a serially concatenated noncoherent system with channel coherence length T, the mutual information is bounded by

$$I_{\mathcal{M}}(SNR) = \log_2(M)\frac{T-1}{T}\int A(u, SNR)du, \qquad (8)$$

where A denotes the demodulator EXIT function for a given SNR.

Proof: We apply the EXIT chart area property, which states that the rate of the outer decoder equals the area under its exit curve, B^{-1}. This implies that the best possible (typically unrealizable) choice of outer code is when the decoder curve perfectly matches the inner demodulator curve at convergence. Thus, the highest possible rate of the outer code for convergence at a given SNR is the area under the demodulator curve at that SNR. □

Figure 7 compares the noncoherent capacity of 16-QAM with the preceding upper bound on the achievable rate when restricted to using a unit-rate differentially modulated inner code with Gray-like bit maps. The result shows that there is a 1 dB loss for this restriction for the case of an aligned PSK rings alphabet. The loss for a lattice alphabet is around 1.8 dB, depending on the rate.

Finally, we comment on *block differential modulation*, a unit-rate modulation scheme that is an alternative to standard differential modulation. In block differential modulation, information is encoded in transitions in amplitude and phase relative to a fixed symbol: in practice, the reference symbol might be the first symbol of the current block, which would be the same as the last symbol of the previous block, if successive blocks overlap by a symbol. For turbo noncoherent

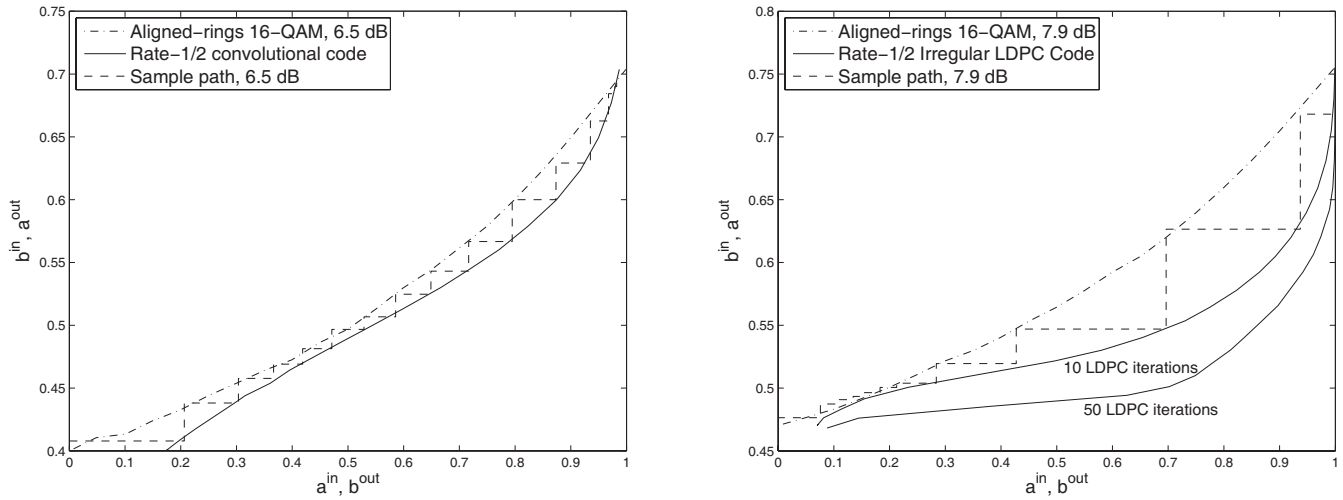

(a) Standard convolutional code.

(b) Irregular LDPC code.

Fig. 8. Rate-1/2 channel codes with 16-QAM and block noncoherent demodulation.

communication with QPSK alphabets [4], block differential modulation was found to yield the same convergence threshold when paired with a turbo-like code as standard differential modulation paired with a convolutional code. However, as mentioned earlier, demodulation for block differential modulation is significantly more complex, requiring phase quantization over $[0, 2\pi]$, compared to the much smaller interval required for standard differential modulation. Furthermore, the bootstrap mechanism that we employ for amplitude estimation using standard differential modulation does not work well with block differential modulation. A possible explanation is that there is less averaging in the amplitude estimator for block differential modulation, since the fixed reference symbol must always be involved.

VI. Channel Coding for Noncoherent Modulation

Given the constellation and bit-mapping, modified EXIT charts guide the appropriate choice of outer channel code. Figure 8 compares the EXIT functions of aligned PSK rings 16-QAM at (a) 6.5 dB when paired with a standard rate-1/2 convolutional code with generator polynomial $G = [23\ 35]$ and (b) 7.9 dB when paired with rate-1/2 irregular LDPC code optimized for the AWGN channel [16]. In both cases, the information rate is 1.8 bits per channel symbol. The number of LDPC decoder iterations used to generate a sample path is 10.

Figure 8 demonstrates that a standard convolutional code is well-matched to unit-rate aligned-rings 16-QAM, yielding at least 1 dB performance improvement from the irregular LDPC code. Note that optimization of the LDPC degree sequence for the specific context of noncoherent demodulation with block fading channel can potentially close this gap. We claim, however, that convolutional coding is near-optimal for the noncoherent amplitude/phase modulation. Taking 6.5 dB (E_b/N_0) as the approximate convergence threshold, as shown in Figure 8(a), and comparing to the modulation code bound for aligned rings 16-QAM (Figure 7), $I_{\mathcal{M}}^{-1}(1.8 \text{ bits/symbol}) = 6.0$ dB (E_b/N_0), we observe that an optimized irregular code could improve the convergence threshold by at most 0.5 dB. Note that the gain for optimizing the LDPC code would be the same (with respect to the depicted convolutional code). Since achieving the modulation code bound requires infinitely many demodulation and decoding iterations (by definition the decoder transfer function is perfectly matched and coincident with the demodulator function), we infer that the convolutional code is is near-optimal for a unit-rate differential modulation code.

VII. Results and Discussion

We first consider simulated BER performance of the aligned-rings 16-QAM constellation with unit-rate Gray-like differential modulation and the standard rate-1/2 convolutional code, shown in Figure 9. The angle of rotational invariance, ϕ, is $\pi/4$ for aligned PSK rings 16-QAM constellation. The full complexity noncoherent receiver and the first iteration of the reduced complexity receiver employ $Q = 5$ phase quantization bins, $\{\phi q/Q\}_{q=0}^{Q-1}$, which is found to closely approximate the performance with an arbitrary number of quantization levels. The overall codeword length is 64,000 bits. Accounting for a $1/T$ rate-loss for differential modulation with i.i.d. block fading, at a coherence length of $T = 10$, the corresponding data rate is 1.8 bits per channel symbol. Noncoherent capacity computations, in Figure 4, show a 1.5 dB advantage for 16-ary amplitude/phase constellations over 16-PSK at this rate. The aligned PSK rings constellation achieves this theoretical advantage. The system is operating around 1.7 dB from capacity, as measured at a BER of 10^{-4}. The gap to capacity is supported with the EXIT analysis of Sections V and VI, which attributes roughly 1 dB for the use of unit-rate modulation and 0.5 dB for non-ideal channel coding. The EXIT chart based convergence threshold estimate is found to be slightly optimistic due to the variability of block fading channel realizations. Finally, there is a small loss of 0.1 dB in the reduced complexity receiver for GLRT based selection of the best two phase branches.

We further compare the performance to a coded *coherent* transceiver with Gray-coded 16-QAM (lattice constellation) and the block fading channel. For this purpose, one symbol

TABLE I
INFORMATION RATES ATTAINED USING TURBO DESIGNS BASED ON ALIGNED PSK RINGS WITH GAP TO CAPACITY AND IMPROVEMENT OVER PSK

Bits/channel use	Constellation size	Outer code rate	Gap to capacity (dB)	Improvement over PSK (dB)
0.675	8	1/4	1.8	-0.2
1.35	8	1/2	1.8	0.4
1.35	16	3/8	1.8	1
1.8	16	1/2	1.7	1.5

per T channel symbols is used as a pilot. The ratio of pilot energy to total energy over a block of symbols is optimized using the BER, and is found to be 25% for the case of one pilot symbol and $T = 10$. The case of multiple pilots with rate matched outer codes was also considered, but did not perform as well for the studied coherence length. The irregular LDPC codes were constructed using a Progressive Edge Growth (PEG) algorithm (see [17]) according to asymptotically optimal degree distributions for the AWGN channel [18]. The codeword length is 64,000 bits and information rate is 1.8 bits/symbol. The BER curve corresponding to 100 LDPC iterations is depicted in Figure 9. This comparison shows the advantage of noncoherent techniques for the SNR regime considered. In particular, for large QAM constellations, where the SNR is large, the cost of channel estimation significantly impacts performance in moderate-to-fast fading channels. The simulation results provided, for idealized block fading channels, show that practical noncoherent systems are able to improve performance by 1 dB.

Table I summarizes the computer simulation results, and indicates that serial concatenation of a convolutional code and differential amplitude/phase modulation approaches Shannon capacity for a block fading channel model, and performs significantly better than DPSK for moderately high SNRs and constellation sizes of 16 or larger. We have developed modified EXIT analysis tools for constellation and bit mapping choice, and for matching outer and inner codes. An important potential application is to the design of OFDM-based fourth generation wireless cellular systems: the complexity of our turbo noncoherent system is comparable to that of coherent systems with turbo-like coded modulation, so that noncoherent architectures are now implementable. However, we are still about 1.8 dB from capacity for an information rate of 1.8 bits/symbol, using a 16-ary amplitude/phase constellation. Since the convolutional outer code appears to be near-optimal if unit-rate differential modulation is used as the inner code, one possible approach to close the gap may be to employ a lower rate inner code, alleviating the 1 dB loss for unit-rate modulation assigned by the modulation code bound (8). Other approaches include suitably optimizing the degree distribution of an LDPC outer code, with different possible choices of inner modulation code. It is also important to quantify how much of the gap to capacity can be closed simply by increasing the code length, or by increasing the constellation size and decreasing the outer code rate, while still employing a unit-rate inner differential modulator.

In practice, the fading gain for a mobile channel varies continuously with time. However, the block-wise constant approximation for channel gains works well for the settings found in current and projected commercial digital cellular systems. For example, block fading models are well-suited for channels that arise in frequency hopping or Hybrid-ARQ systems. Further, we conjecture that, with appropriate choice of coherence length, the capacity of the block fading model should be close to that of a continuously varying channel for SNRs typical of practical systems. It is of interest to give precise shape to this intuition in the context of a specific continuously varying channel model.

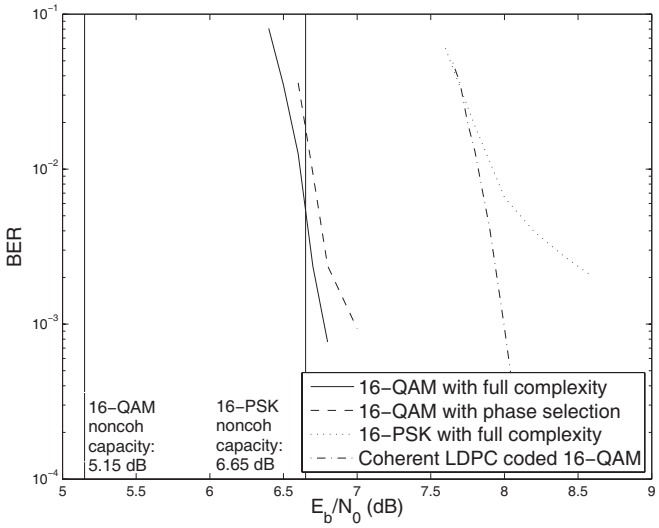

Fig. 9. Performance of coded noncoherent 16-QAM receivers with Rayleigh block fading, channel $T = 10$. Approximately 1.5 dB is gained over the equivalent noncoherent 16-PSK system. Also shown is the performance of a coherent LDPC coded 16-QAM transceiver in which the number and power ratio of the pilots is optimized.

While we have considered relatively small normalized Doppler frequencies (where the normalization is relative to the symbol rate) typical of outdoor cellular wireless systems, there are other situations in which the normalized Doppler may be large enough that a block fading approximation breaks down even at low SNR. It is of interest to explore alternative structures for turbo noncoherent communication in such settings, with preliminary work in this direction reported in [19], [9].

REFERENCES

[1] R.-R. Chen, D. Agrawal, and U. Madhow, "Noncoherent detection of factor-graph codes over fading channels," in *Proc. IEEE Conf. on Inf. Sciences and Systems (CISS)*, Princeton, NJ, USA, Mar. 2000.

[2] M. Peleg, S. Shamai, and S. Galán, "Iterative decoding for coded noncoherent MPSK communications over phase-noisy AWGN channel," *IEE Proc. Commun.*, vol. 147, no. 2, pp. 87–95, Apr. 2000.

[3] P. Hoeher and J. Lodge, "Turbo DPSK: iterative differential PSK demodulation and channel decoding," *IEEE Trans. Commun.*, vol. 47, no. 6, pp. 837–842, June 1999.

[4] R.-R. Chen, R. Koetter, D. Agrawal, and U. Madhow, "Joint demodulation and decoding for the noncoherent block fading channel: a practical framework for approaching channel capacity," *IEEE Trans. Commun.*, vol. 51, no. 10, pp. 1676–1689, Oct. 2003.

[5] I. Motedayen-Aval and A. Anastasopoulos, "Polynomial-complexity noncoherent symbol-by-symbol detection with application to adaptive iterative decoding of turbo-like codes," *IEEE Trans. Commun.*, vol. 51, no. 2, pp. 197–207, Feb. 2003.
[6] D. Warrier and U. Madhow, "Spectrally efficient noncoherent communication," *IEEE Trans. Inform. Theory*, vol. 48, no. 3, pp. 651–668, Mar. 2002.
[7] O. Macchi and L. Scharf, "A dynamic programming algorithm for phase estimation and data decoding on random phase channels," *IEEE Trans. Inform. Theory*, Sept. 1981.
[8] T. Marzetta and B. Hochwald, "Capacity of a mobile multiple-antenna communication link in Rayleigh flat fading," *IEEE Trans. Inform. Theory*, vol. 45, no. 1, pp. 139–157, Jan. 1999.
[9] R. Nuriyev and A. Anastasopoulos, "Capacity characterization for the noncoherent block-independent AWGN channel," in *Proc. IEEE International Sym. on Inf. Theory (ISIT)*, Yokohama, Japan, July 2003.
[10] L. Zheng and D. Tse, "Communicating on the Grassmann manifold: a geometric approach to the non-coherent multiple antenna channel," *IEEE Trans. Inform. Theory*, vol. 48, no. 2, pp. 359–383, Feb. 2002.
[11] L. Bahl, J. Cocke, F. Jelinek, and J. Raviv, "Optimal decoding of linear codes for minimizing symbol error rate," *IEEE Trans. Inform. Theory*, vol. 20, pp. 284–287, Mar. 1974.
[12] S. ten Brink, "Convergence behavior of iteratively decoded parallel concatenated codes," *IEEE Trans. Commun.*, vol. 49, no. 10, pp. 1727–1737, Oct. 2001.
[13] M. Tüchler and J. Hagenauer, "EXIT charts of irregular codes," in *Proc. IEEE Conf. on Inf. Sciences and Systems (CISS)*, Princeton, NJ, USA, Mar. 2002.
[14] A. Ashikhmin, G. Kramer, and S. ten Brink, "Extrinsic information transfer functions: model and erasure channel properties," *IEEE Trans. Inform. Theory*, vol. 50, no. 11, pp. 2657–2673, Nov. 2004.
[15] J. Proakis, *Digital Communications*. New York: McGraw-Hill International Editions, 1995.
[16] T. Richardson, M. Shokrollahi, and R. Urbanke, "Design of capacity-approaching irregular low-density parity-check codes," *IEEE Trans. Inform. Theory*, vol. 47, no. 2, pp. 619–637, Feb. 2001.
[17] N. Jacobsen and R. Soni, "Design of rate-compatible irregular LDPC codes based on edge growth and parity splitting," in *Proc. IEEE Vehicular Tech. Conf. (VTC)*, Baltimore, MD, Sept. 2007.
[18] T. Richardson and R. Urbanke, "The capacity of low-density parity-check codes under message-passing decoding," *IEEE Trans. Inform. Theory*, vol. 47, no. 2, pp. 599–618, Feb. 2001.
[19] R.-R. Chen, R. Koetter, and U. Madhow, "Joint noncoherent demodulation and decoding for fast Rayleigh fading channels," in *Proc. IEEE Conf. on Inf. Sciences and Systems (CISS)*, Baltimore, MD, USA, Mar. 2003.

Noah Jacobsen received the B.S. degree in Electrical Engineering from Cornell University, Ithaca, NY in 2000, and the M.S. and Ph.D. degrees in Electrical and Computer Engineering from the University of California, Santa Barbara in 2005. He is currently with Alcatel-Lucent, Murray Hill, New Jersey.

Upamanyu Madhow is a Professor of Electrical and Computer Engineering at the University of California, Santa Barbara. His research interests are in communication systems and networking, with current emphasis on wireless communication, sensor networks and multimedia security. He received his bachelor's degree in electrical engineering from the Indian Institute of Technology, Kanpur, in 1985, and his Ph. D. degree in electrical engineering from the University of Illinois, Urbana-Champaign in 1990. He has worked as a research scientist at Bell Communications Research, Morristown, NJ, and as a faculty at the University of Illinois, Urbana-Champaign. Dr. Madhow is a recipient of the NSF CAREER award. He has served as Associate Editor for Spread Spectrum for the IEEE TRANSACTIONS ON COMMUNICATIONS, and as Associate Editor for Detection and Estimation for the IEEE TRANSACTIONS ON INFORMATION THEORY. He currently serves as Associate Editor for the IEEE TRANSACTIONS ON INFORMATION FORENSICS AND SECURITY. He is the author of the textbook *Fundamentals of Digital Communication,* published by Cambridge University Press in 2008.